Phase behaviors in a binary mixture of diblock copolymers confined between two parallel walls*

Pan Jun-Xing(潘俊星), Zhang Jin-Jun(张进军)†, Wang Bao-Feng(王宝凤), Wu Hai-Shun(武海顺), and Sun Min-Na(孙敏娜)

School of Chemistry and Materials Science, Shanxi Normal University, Linfen 041004, *China*

(Received 14 April 2012; revised manuscript received 9 July 2012)

The phase behaviors in a binary mixture of diblock copolymers confined between two parallel walls are investigated by using a cell dynamics simulation of the time-dependent Ginzburg–Landau theory. The morphological dependence of the wall-block interaction and the distance between walls (confinement degree) has been systematically studied, and the effect of repulsive interactions between different monomers is also discussed. It is interesting that multiple novel morphological transitions are observed by changing these factors, and various multilayered sandwich structures are formed in the mixture. Furthermore, the parametric dependence and physical reasons for the microdomain growth and orientational order transitions are discussed. From the simulation, we find that much richer morphologies can form in a binary mixture of diblock copolymers than those in a pure diblock copolymer. Our results provide an insight into the phase behaviors under parallel wall confinement and may provide guidance for experimentalists. This model system can also give a simple way to realize orientational order transition in soft materials through confinement.

Keywords: parallel walls confinement, phase behavior, binary mixture, diblock copolymer

PACS: 64.75.Va, 64.75.Yz, 83.80.Uv, 83.80.Tc **DOI:** 10.1088/1674-1056/22/2/026401

1. Introduction

Self-assembly in soft matter systems is a powerful method for creating novel phase structures on the nanoscale. Polymeric materials with novel structures can exhibit novel physical properties and have a variety of potential applications, such as nanolithography, fabrication of nanoporous membranes for advanced separation media, and photonic crystals.[1–4] The phase separations in block copolymers and multi-component mixtures have been a hot topic both experimentally[5–12] and theoretically[13–18] due to their potential importance in materials engineering.

However, the problem of using block copolymers is how to control their nanostructure. There are a large number of experimental and theoretical works which address the problem of tailoring a desired nanostructure. Applied external fields are promising candidates to achieve that goal.[19] Such fields can be an electric field,[20–26] shear flow,[27–31] and surface fields.[32–38] By using self-consistent field theory, Matsen has examined the undulation mode in films of parallel lamellae and calculated the critical electric field, beyond which the mode becomes unstable.[20] Recently, our group has also investigated the orientational order transition of striped patterns in microphase structures of diblock copolymer–diblock copolymer mixtures in the presence of periodic oscillatory particles.[22] Moreover, Morozov and coworkers have produced many works about the shear-induced phase transitions in polymer mixtures.[28–30] Surface fields are, in particular, prominent in confined geometries, such as parallel wall confinement,[39–57] nano-cylinder tube confinement,[57–70] and spherical confinement.[57,71–75] In experimental studies, Kellogg, Walton, and Mayes have studied the specificity of block-wall interactions of diblock copolymer films confined between parallel walls; they observed that for highly specific interactions, one block component segregates to both interfaces, and the frustration due to incommensuration between film thickness and the diblock's bulk period is accommodated by the formation of layers parallel to the walls with a perturbed period; in contrast, reduced specific interactions allow the frustration to be accommodated by perpendicular ordering of the diblock, such that both block components are present at the walls.[45] Further experiments have also revealed that lamellae parallel to surfaces appear in a symmetric diblock copolymer confined between walls which preferentially attract one of the two blocks.[46,47] In theoretical studies, Chen and Chakrabati presented results from a numerical study of a coarse-grained model of diblock copolymer thin films confined between hard walls.[48] Using self-consistent field theory, Pickett and Balazs have studied the microdomain morphologies of diblock copolymers when they are confined between two neutral or attractive plates. Their results indicated that a lamella phase occurs in both cases, and that the lamellae are perpendicular to the plates if neutral walls are adopted; and then it turns to

*Project supported by the National Natural Science Foundation of China (Grant No. 20673070), the Natural Science Foundation of Shanxi Province (Grant No. 2007011055), the Natural Science Foundation for Young Scientists of Shanxi Province (Grant No. 2011021008-1), and the Soft Science Program of Shanxi Province (Grant No. 2011041015-01).

†Corresponding author. E-mail: zhangjinjun@sxnu.edu.cn

© 2013 Chinese Physical Society and IOP Publishing Ltd

parallel to the plates when the attractive strength is added.[49] Recently, Feng, Liu, and Hu have performed Monte Carlo simulations and used the cell dynamics simulation method (CDS) to investigate the microphase separation and morphology of symmetric and asymmetric diblock copolymer thin films confined in a slit with neutral or attractive surfaces, and they found that when the walls are neutral, a parallel ordered lamella structure only exists over a short range, while irregular microdomain morphology occurs over the whole region; when directional quenching is applied, or the walls are attractive to one of the blocks, a periodical lamellar structure of alternating *A*-rich and *B*-rich layers occurs over the whole region of the film, and the change of slit width and interaction strength will influence the period and arrangement of the lamella.[52,53]

Up to now, most studies have focused on the pure block copolymers under confinement. In this paper, we systematically investigate the phase behaviors of a diblock copolymer mixture under parallel wall confinement by using the cell dynamics simulation of the time-dependent Ginzburg–Landau theory proposed by Oono and co-workers.[76–78] Novel self-assembled structures are expected to be observed in such a system. The paper is organized as follows: in Section 2, we describe the experimental model and CDS method; the results and discussion are presented in Section 3, we discuss the effects of wall-block interaction, walls confinement degree, and repulsive interactions between different monomers on the phase separation; conclusions are drawn in Section 4.

2. Model and simulation method

We consider a binary mixture system of two different *AB* and *CD* diblock copolymers confined between two parallel, smooth and impenetrable walls. The walls locate at the y direction. Here, we use the x and y axes to stand for the horizontal and vertical directions, respectively. There is a short-range repulsive interaction between two kinds of copolymer chains in each diblock copolymer. The monomers in *AB* and *CD* copolymers are mutually incompatible. Moreover, in the present model we ignore the hydrodynamic effects, because they just play a role in a very late stage of phase separation in polymer blends.

The polymerization degrees of *A*, *B*, *C*, and *D* blocks are N_A, N_B, N_C, and N_D, respectively. In this paper, we assume that the polymerization degrees of *A* and *B* blocks are equal ($N_A = N_B$), and they are also the same for *C* and *D* blocks ($N_C = N_D$). The interaction between monomers i and j is denoted by the Flory–Huggins parameter χ_{ij}, where $i, j = A$, *B*, *C*, and *D*. ϕ_A, ϕ_B, ϕ_C, and ϕ_D are the local volume fractions of these monomers. Under the incompressibility condition, the total density $\phi_A + \phi_B + \phi_C + \phi_D$ is constant, so we take $\psi = \phi_A + \phi_B$, $\phi = \phi_A - \phi_B$, and $\xi = \phi_C - \phi_D$ as the independent variables, which are similar to our previous work.[22,36] These three quantities are the order parameters to describe the phase behavior of the system. Among them, ψ reflects the segregation of binary mixture, whereas ϕ and ξ are the local concentration differences between monomers *A* and *B* and between monomers *C* and *D*, respectively.

For the binary mixture system of two diblock copolymers, the free-energy function is

$$F = F_{\mathrm{L}} + F_{\mathrm{S}}, \tag{1}$$

the long-range part F_{L} is given by

$$F_{\mathrm{L}} = \frac{\alpha}{2}\iint \mathrm{d}\boldsymbol{r}\mathrm{d}\boldsymbol{r}' G(\boldsymbol{r},\boldsymbol{r}')[\phi(\boldsymbol{r})-\phi_0][\phi(\boldsymbol{r}')-\phi_0] + \frac{\beta}{2}\iint \mathrm{d}\boldsymbol{r}\mathrm{d}\boldsymbol{r}' G(\boldsymbol{r},\boldsymbol{r}')[\xi(\boldsymbol{r})-\xi_0][\xi(\boldsymbol{r}')-\xi_0], \tag{2}$$

where α and β are positive constants corresponding to the polymerization degrees of *AB* copolymer (N_{AB}) and *CD* copolymer (N_{CD}). $G(\boldsymbol{r},\boldsymbol{r}')$ is the Green function defined by the equation $-\nabla^2 G(\boldsymbol{r},\boldsymbol{r}') = \delta(\boldsymbol{r}-\boldsymbol{r}')$, while ϕ_0 and ξ_0 are the spatial averages of ϕ and ξ, respectively. In the case of symmetric diblock copolymers, $\phi_0 = 0$, and $\xi_0 = 0$. In contrast to the long-range part, the short-range part F_{S} is a little more complicated and is given by the equation,[52,53,79]

$$F_{\mathrm{S}} = \iint \mathrm{d}x\mathrm{d}y\left[\frac{d_1}{2}(\nabla\psi)^2 + \frac{d_2}{2}(\nabla\phi)^2 + \frac{d_3}{2}(\nabla\xi)^2 + f(\psi,\phi,\xi) - s(y)\phi\right], \tag{3}$$

here, d_1, d_2, and d_3 terms correspond to the surface tensions, and the last term on the right is the surface field of the wall-block interaction.[79] Furthermore, we use $\eta = \psi - \psi_{\mathrm{c}}$ instead of ψ,[18,21,22,34,80,81] where ψ_{c} is the volume fraction at the critical point of the macrophase separation of two different copolymers. It is obtained as $\psi_{\mathrm{c}} = N_C^{1/2}/(N_A^{1/2} + N_C^{1/2})$. The local interaction term $f(\eta,\phi,\xi)$ is

$$f(\eta,\phi,\xi) = \left(-\frac{1}{2}c_1\eta^2 + \frac{1}{4}\mu_1\eta^4\right) + \left(-\frac{1}{2}c_2\phi^2 + \frac{1}{4}\mu_2\phi^4\right) + \left(-\frac{1}{2}c_3\xi^2 + \frac{1}{4}\mu_3\xi^4\right) + b_1\eta\phi - b_{11}\eta\xi - \frac{1}{2}b_2\eta\phi^2 + \frac{1}{2}b_{22}\eta\xi^2. \tag{4}$$

The important physical results will be mainly included in it. In our model, we choose two kinds of symmetric diblock copolymers, so the $\eta^2\phi$ term and the $\eta^2\xi$ term will vanish. In Eq. (4), all the coefficients c's, μ's, and b's are determined, for example, $b_1 = \frac{1}{4}[-\chi_{AC} - \chi_{AD} + \chi_{BC} + \chi_{BD}]$, $b_{11} = \frac{1}{4}[-\chi_{AC} + \chi_{AD} - \chi_{BC} + \chi_{BD}]$, $b_2 = b_{22} = (N_A^{-1/2} + N_C^{-1/2})^2$, for $N_A = N_B$ and $N_C = N_D$. The b_1 term and b_{11} term originate from the short-range interactions between monomers, whereas the b_2 term and b_{22} term arise from the conformation entropy of the copolymers. Here, we choose $b_1 > 0$ and $b_{11} > 0$, so that there is a relatively large repulsive interaction

between monomers B and D. Equation (4) prescribes the minimal model of the short-range part of the free energy in our system. From the b_2 term and b_{22} term, one can see that a microphase separation could occur in the copolymers. In fact, the b_2 term implies that a large absolute value of ϕ is favorable in the region $\eta > 0$, whereas the b_{22} term means that a large absolute value of ξ is more favorable in the region $\eta < 0$. Competitive interactions in the free-energy functional will lead to phase separations in our diblock copolymers mixture.

In terms of the free-energy functions in Eqs. (1)–(4), the coupled equations for the three order parameters are

$$\frac{\partial \eta}{\partial t} = M_\eta \nabla^2 \frac{\delta F}{\delta \eta}, \tag{5}$$

$$\frac{\partial \phi}{\partial t} = M_\phi \nabla^2 \frac{\delta F}{\delta \phi}, \tag{6}$$

$$\frac{\partial \xi}{\partial t} = M_\xi \nabla^2 \frac{\delta F}{\delta \xi}, \tag{7}$$

where M_η, M_ϕ, and M_ξ are the positive transport coefficients. We carry out the numerical solutions of the above model system in an $L \times L$ two-dimensional square lattice by using the cell dynamics simulation (CDS) approach. The CDS equations corresponding to Eqs. (5)–(7), in their space-time discretized forms, are written as follows:

$$\eta(\boldsymbol{r}, t+\Delta t) = \eta(\boldsymbol{r}, t) + M_\eta(\langle\langle I_\eta \rangle\rangle - I_\eta), \tag{8}$$

$$\phi(\boldsymbol{r}, t+\Delta t) = \phi(\boldsymbol{r}, t) + M_\phi\{(\langle\langle I_\phi \rangle\rangle - I_\phi) - \alpha[\phi(\boldsymbol{r}, t) - \phi_0]\}, \tag{9}$$

$$\xi(\boldsymbol{r}, t+\Delta t) = \xi(\boldsymbol{r}, t) + M_\xi\{(\langle\langle I_\xi \rangle\rangle - I_\xi) - \beta[\xi(\boldsymbol{r}, t) - \xi_0]\}, \tag{10}$$

where

$$I_\eta = -d_1(\langle\langle \eta \rangle\rangle - \eta) - A_\eta \tanh \eta + \eta + b_1\phi - b_{11}\xi - \frac{1}{2}b_2\phi^2 + \frac{1}{2}b_{22}\xi^2, \tag{11}$$

$$I_\phi = -d_2(\langle\langle \phi \rangle\rangle - \phi) - A_\phi \tanh \phi + \phi + b_1\eta - b_2\eta\phi - s(y), \tag{12}$$

$$I_\xi = -d_3(\langle\langle \xi \rangle\rangle - \xi) - A_\xi \tanh \xi + \xi - b_{11}\eta + b_{22}\eta\xi, \tag{13}$$

and

$$\langle\langle X \rangle\rangle = \frac{1}{6}\sum_{NN} X + \frac{1}{12}\sum_{NNN} X. \tag{14}$$

The subscripts NN and NNN stand for the nearest-neighbor and next-nearest-neighbor cells, respectively. In Eq. (12), the last term $s(y)$ is written as follows:

$$s(y) = H_i \times (\delta_{1,y} + \delta_{L_y,y}). \tag{15}$$

Here, i denotes the attractive bead; H_i is the strength of wall-block interaction. We choose $H_A > 0$ for A-block attractive walls, $H_B < 0$ for B-block attractive walls, and $H = 0$ for neutral walls. In this paper, we just consider the neutral and A-block attractive walls, and we can expect that the results of B-block attractive walls are similar to A-block attractive walls. $\delta_{1,y}$ and $\delta_{L_y,y}$ are Kronecker delta.

For the diblock copolymers mixture confined between two hard parallel walls in this work, we adopt the boundary conditions presented by Marko.[79] The periodic boundary conditions are applied in the x direction and boundary conditions in the y direction are set as follows:

$$X(x, 0, t) = X(x, 1, t), \tag{16}$$

$$X(x, L_y + 1, t) = X(x, L_y, t). \tag{17}$$

Our ensuing simulations of the model system are performed by choosing the parameters with $L_x = L_y = 128$, $A_\eta = 1.3$, $A_\phi = 1.1$, $A_\xi = 1.1$, $d_1 = 1.0$, $d_2 = 0.5$, $d_3 = 0.5$, $\phi_0 = 0$, $\xi_0 = 0$, $b_2 = 0.2$, $b_{22} = 0.2$, $b_1 = 0.09$, and $M_\eta = M_\phi = M_\xi = 1$, the initial distribution of η, ϕ, ξ, are specified by random uniform distributions in the range $[-0.01, 0.01]$. For the original cell dynamics simulation, the lattice size (Δx or Δy) are set to be 1, and the time step (Δt) is set to be 0.8. In this paper, all parameters are scaled, so all of them are dimensionless.[76] In the present simulation work, in the case of $\alpha = 0.04$, $\beta = 0.03$, by the formula $\alpha = 12/[N^2 f_b(1 - f_b)]$ (f_b denotes a block ratio),[82] one can obtain that $N_A = N_B = 17$, $N_C = N_D = 20$, $\chi_{AB}N_{AB} = 15.05$, and $\chi_{CD}N_{CD} = 16$, where $N_{AB} = N_A + N_B$ and $N_{CD} = N_C + N_D$.

3. Numerical results and discussion

3.1. Wall-block interaction effect on the ordering of the mixture

In this section, we investigate the orientational order transition of microphase structures in diblock copolymers with wall-block attractive strength H_A increasing. Figure 1 shows several typical equilibrium patterns with $f = 51.7/48.3$ (f means the composition ratio of AB diblock copolymer and CD diblock copolymer) at time $t = 5 \times 10^6$, when the attractive strength H_A increases from 0 to 1.0 step by step. The parameter b_{11} is set to 0.099.

From Fig. 1 we can see that in the absence of walls confinement, the overall macro-morphology is isotropic. The CD diblock copolymer domains are surrounded by an AB diblock copolymer, while the micro-morphology of both copolymers is lamellar (Fig. 1(a)). When the mixture is confined between two neutral parallel walls in the y direction, the microdomains of both AB and CD diblock copolymers are ordered along the direction perpendicular to the walls (Fig. 1(b)). When the walls have a weak attractive effect on the A monomer, the stable morphology of the two polymers is broken, and the striped structure begins to bend, both AB and CD diblock copolymers reverse from perpendicular to parallel to the walls, shown

in Fig. 1(c). As the wall–block attractive strength increasing, the parallel morphology of the two copolymers become larger, as shown in Fig. 1(d). When the attractive strength is large enough, a complete phase morphology reversal of *AB* and *CD* copolymers occurs, both copolymers are all parallel to the walls, and a perfect sandwich structure with *AB*-rich and *CD*-rich striped structure alternating forms finally, as shown in Fig. 1(e).

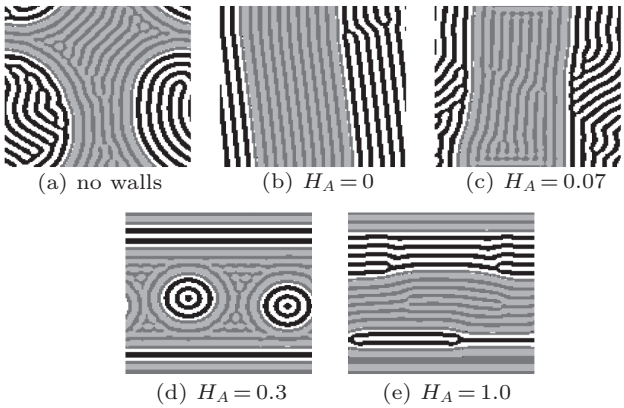


Fig. 1. Pattern evolution of a 128×128 two-dimensional lattice with $f = 51.7/48.3$ at time $t = 5 \times 10^6$. Phase *A* is represented by the gray region, phase *B* by the light gray region, phase *C* by the white region, and phase *D* by the black region.

From the above result, we can find the following explanations. When the binary mixture of *AB* diblock copolymer and *CD* diblock copolymer is asymmetric, the minority *CD* diblock copolymer will form islands in the majority *AB* diblock copolymer, and this has already been proved by our previous works.[18,22] Furthermore, the incompatibility and the short-range interactions of different monomers causes different block copolymers to form micro-level striped structures (Fig. 1(a)). When the system is confined between two neutral walls, because the distance between walls that we chose is incommensurate with the natural period of the lamellae (L_0), the effect of wall confinement means that the copolymer chains cannot extend freely along the direction perpendicular to the walls. The rule of the free energy minimization drives the mixture to form an ordered striped structure in the direction perpendicular to the walls, so that the copolymer chains can extend in the largest region (Fig. 1(b)). We will discuss the effect of the wall confinement degree in detail later. When the walls have a weak selective attraction to block *A*, monomer *A* begins to gather on the walls, the original ordered structure is disrupted, the *AB* block copolymer begins to reverse from the perpendicular layered structure to a parallel structure in the direction of walls, and the *CD* block copolymer also begins to reverse from the perpendicular layered structure to a parallel structure due to the repulsive interactions between different monomers. In the end, a mixed structure with the layers parallel and perpendicular to the walls in the two copolymers forms (Fig. 1(c)). In addition, because the wall–block attraction is a short-range interaction, the phase separation process of the parts far from the walls is slower than the parts close to the walls (Fig. 1(d)). When the wall–block attraction is large enough, more *A* monomers cover the surfaces of the walls, and change the composition ratio of the *AB* diblock copolymer and the *CD* diblock copolymer in the middle part, so that both *AB* and *CD* copolymers in the whole range are parallel to the walls, and a multilayered sandwich structure forms (Fig. 1(e)). The phase transition of Fig. 1(d) and Fig. 1(e) can be seen clearly in Fig. 2.

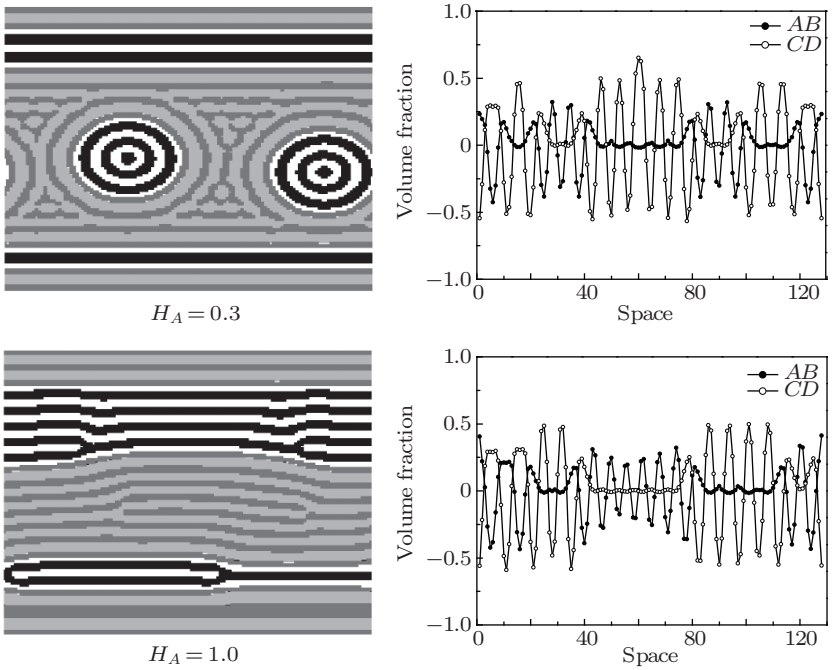


Fig. 2. The figures on the left-hand side are the domain patterns for $H_A = 0.3$ and $H_A = 1.0$ at $t = 5 \times 10^6$. The color details are the same as those in Fig. 1. The figures on the right-hand side display the volume fractions profile of ϕ (*AB*) and ξ (*CD*) along the line $x = 43$.

Figure 2 shows the volume fractions profile of $\phi(AB)$ and $\xi(CD)$ along the line $x = 43$. We can see that with the wall–block interaction changing from 0.3 to 1.0, the volume fractions profiles of *AB* blocks and *CD* blocks change greatly. This indicates that the wall–block interaction influences the distribution of *AB* and *CD* copolymers in the middle part.

In summary, when the diblock copolymers mixture is confined between two parallel walls, the morphology of the mixture changes from isotropic to perpendicular to the walls and then to parallel to the walls with the wall–block interaction increasing, and a perfect parallel multilayered sandwich structure forms in the end. The results provide a simple way to realize the orientational transition in a copolymer mixture by selecting different property substrates experimentally.

Furthermore, we study the domain growth of *A*, *B*, *C*, and *D* blocks by investigating the pattern evolution with time. Figure 3 displays the domain growth with $f = 51.7/48.3$, $b_{11} = 0.099$, and $H_A = 1.0$, corresponding to Fig. 1(e).

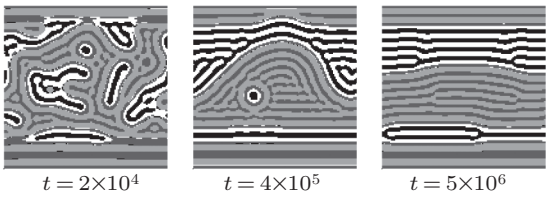


Fig. 3. Domain growth of a 128×128 two-dimensional lattice with $f = 51.7/48.3$, $b_{11} = 0.099$, and $H_A = 1.0$. Other details are the same as those in Fig. 1.

Figure 3 shows that at the early stage (about $t = 2 \times 10^4$), the macrophase separation occurs whereas the microdomain growth is weak; as $t = 4 \times 10^5$, the microphase separation takes place obviously, and the growth of microdomains is more rapid than that of macrodomains, and the effect of wall–block interaction begins to appear; at the late stage, $t = 5 \times 10^6$, both the highly orientational ordered microdomains and macrodomains form in the mixture. We find that a well striped structure along the x direction has emerged in the long-range process.

To consider this case in greater depth, we study the effect of the wall–block attractive strength on the microdomain growth of the *AB* copolymer by calculating numerically the domain size $R_i(t)$ ($i = x$ or y) in the x and y directions as a function of time,

$$R_i(t) = 2\pi/\langle k_i(t)\rangle, \tag{18}$$

where

$$\langle k_i(t)\rangle = \int \mathrm{d}\boldsymbol{k}\, k_i S(\boldsymbol{k},t) \Big/ \int \mathrm{d}\boldsymbol{k}\, S(\boldsymbol{k},t). \tag{19}$$

Here, $S(\boldsymbol{k},t)$ is the structure factor which is determined by the Fourier component of the spatial concentration distribution $\phi(\boldsymbol{r},t)$. It is defined by $S(\boldsymbol{k},t) = \langle|\phi(\boldsymbol{k},t)|\rangle^2$.[83] Figure 4 shows the time evolution of *AB* microdomain size $R_i(t)$ in the x and y directions as a function of time in double logarithmic plots. The results are averaged over ten independent runs.

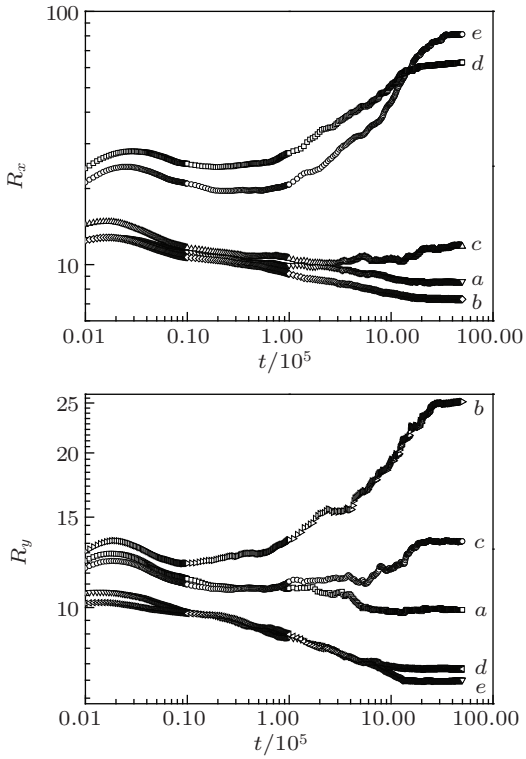


Fig. 4. Time evolution of the characteristic sizes of *AB* diblock copolymer microdomains $R_x(t)$ and $R_y(t)$ for $f = 51.7/48.3$, $b_{11} = 0.099$, and different wall–block interactions. Curve *a*: no walls; curve *b*: $H_A = 0.0$; curve *c*: $H_A = 0.07$; curve *d*: $H_A = 0.3$; curve *e*: $H_A = 1.0$.

From Fig. 4(a), we see that in equilibrium when the mixture is confined between two neutral walls, the *AB* microdomain size R_x decreases (from curves *a* to *b*), and then gradually increases when the wall–block attraction increases. This fact indicates that as the attractive strength increases, the coarsening of microdomains is along the wall direction. Different from Fig. 4(a), figure 4(b) shows that the *AB* microdomain size R_y first increases when the walls are neutral and then decreases with the wall–block attractive strength increasing. It means that as the wall–block attractive strength is strong enough, the coarsening of the *AB* microdomain perpendicular to the wall direction is impeded. In addition, from Fig. 4(a) and Fig. 4(b), we can see that at the early stage, there are few differences between all the curves. It means that at the early stage, the inner interaction is dominant. But at the middle stage, the domain growth is very different between the bulk and the confined systems. It is because that at the middle stage, the effect of wall–block attractive interaction becomes obvious, the competition between the inner interaction and the surface field interaction leads to the sharp change of the domain growth. At the late stage, all the domains are stable.

In order to characterize the orientational order transition of microphase striped domains, we calculate the orientational

order parameter S of the AB copolymer in detail,

$$S = \langle 2\cos^2\theta - 1 \rangle, \tag{20}$$

where θ is the angle between the unit normal vector of a stripe and the unit normal vector in the wall direction.[84] The spatial average takes the value $S = 0$ for an isotropic phase, $S = 1$ for a completely oriented phase parallel to the wall direction, and $S = -1$ for another completely orientational phase perpendicular to the wall direction. Figure 5 shows the variation of the order parameter in a process of orientational order transition.

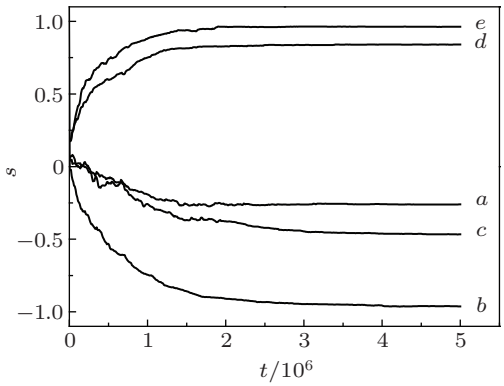


Fig. 5. Alignment kinetics of AB copolymer for different wall–block attractive strength. Curve a: nowalls; curve b: $H_A = 0.0$; curve c: $H_A = 0.07$; curve d: $H_A = 0.3$; curve e: $H_A = 1.0$.

As shown in Fig. 5, the orientational order parameter of AB copolymer first transits from 0 to -1 and then to 1. From curve a, we see that the order parameter S is near to 0, so the AB microphase structure shown in Fig. 1(a) is isotropic due to the inner interaction. When the system is confined between two parallel walls in the y direction, the order parameter S is near to -1 (curve b), it means that the AB microphase structure is perpendicular to the walls. When the walls have a selective attraction on the A block, the value of the order parameter increases obviously (curves b to d) with the wall–block attractive strength increasing. This indicates that AB microdomains coarsen along the direction parallel to the walls. As the attractive strength increases to a suitable value, the order parameter S is near to 1, the AB microphase striped pattern along the walls direction forms, as shown in curve e. Here, the AB microphase structure transits from an isotropic state to a state perpendicular to the wall direction and then to a state parallel to the walls, as shown from Fig. 1(a) to Fig. 1(e). From curves a to e in Fig. 5, we can see that the order parameter S changes basically from 0 to -1 and then to 1. This process is a detailed description of the orientational order transition. In addition, the order parameter S almost has no change at the late stage, so the microphase striped structures we obtain at last are stable.

3.2. Effect of the interactions between different monomers

In order to understand the multilayered sandwich structure further, we examine the dependence of the stable structure on the phenomenological parameter b_{11} in detail, which is determined by the interactions between different blocks in the copolymers, and they are χ_{AC}, χ_{AD}, χ_{BC}, and χ_{BD}. Figure 6 displays the patterns at $t = 5 \times 10^6$ for $f = 51.7/48.3$ with variation of the parameter b_{11} from 0.095 to 0.025, and the value of wall–block attractive strength H_A is 1.0.

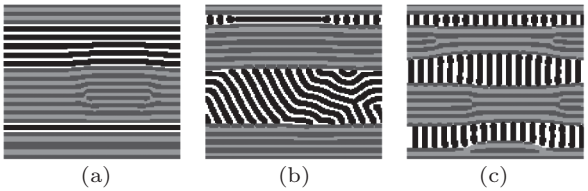


Fig. 6. Pattern evolution of a 128×128 two-dimensional lattice for $f = 51.7/48.3$ with different b_{11} at time $t = 5 \times 10^6$. (a) $b_{11} = 0.095$; (b) $b_{11} = 0.035$; (c) $b_{11} = 0.025$. Other details are the same as those in Fig. 1.

From Fig. 6 we can see that the microdomains of the CD copolymer reverse from parallel to perpendicular to the macrodomain interfaces with b_{11} decreasing, whereas the striped microdomains of AB copolymer are parallel to the macrodomain interfaces at all times.

One can understand the process as follows: on the one hand, because of the strong attractive strength of the walls on the A block, the striped microdomain structure in the AB copolymer does not vary. On the other hand, as we indicated before, the parameter b_{11} represents the repulsive interaction strength of the AB copolymer to the C and D blocks in the CD copolymer. When b_{11} is large enough, that is $\chi_{AD} + \chi_{BD} \gg \chi_{AC} + \chi_{BC}$, it means that the repulsive interaction of the AB copolymer to the D monomer is much larger than the repulsive interaction to the C monomer, so it makes the D monomer not favorable in the macrodomain interfaces. Finally, the C monomer dominates the interfaces of macrophase separation perfectly, resulting in the parallel sandwich patterns (Fig. 6(a)). When b_{11} decreases, the repulsive interaction between the AB copolymer and the D monomer reduces, so the D monomer begins to aggregate to the macrodomain interfaces (Fig. 6(b)). When b_{11} is very small, $\chi_{AD} + \chi_{BD}$ is almost equal to $\chi_{AC} + \chi_{BC}$, so both C and D monomers can aggregate in the macrodomain interfaces, resulting in CD striped microdomains perpendicular to the macrodomain interfaces, and the perpendicular multilayered sandwich structure forms in the end (Fig. 6(c)).

According to the result, we can realize the orientational transition by changing the repulsive interactions between monomers. In experiment, one can achieve the orientational transition by selecting different copolymers.

3.3. Effect of the confinement degree

The phase transition not only can be induced by H_A and b_{11}, but also can be affected by the distance between walls d,

which represents the confinement degree. Firstly, we calculate the natural period of the binary mixture. Figure 7 shows the bulk pattern and the volume fractions on the cross-line of different copolymers with $f = 51.7/48.3$ and $b_{11} = 0.099$.

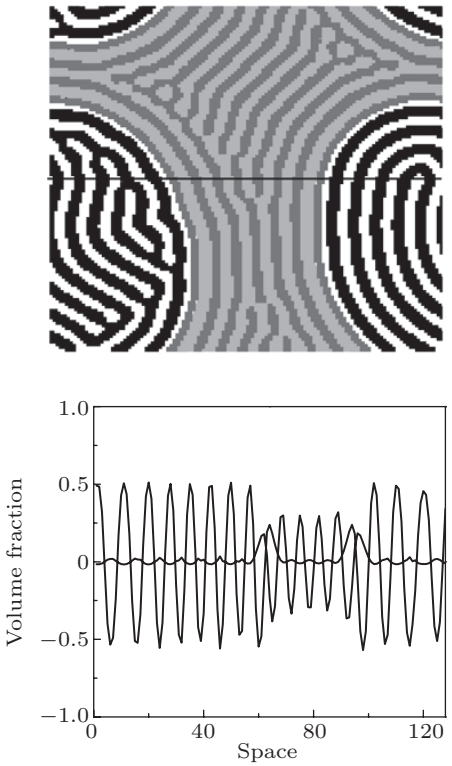


Fig. 7. The figure on the left-hand side is the domain pattern for $f = 51.7/48.3$ and $b_{11} = 0.099$ at $t = 5 \times 10^6$. The color details are the same as those in Fig. 1. The figure on the right-hand side displays the volume fractions profile of ϕ and ξ along the line $y = 64$. The line with the larger amplitude indicates ξ_x, whereas the line with smaller amplitude is ϕ_x.

From Fig. 7 we can see that in the bulk, both *AB* and *CD* copolymers form a layer structure in their own domains. It is widely accepted that the equilibrium mean thickness D of phase-separated microdomains scaled by the degree of polymerization N of the copolymers obeys a power law of the form $D \sim N^{\theta}$ and $\theta = 2/3$ for the strong-segregation limit.[85] Because of the similar degree of polymerization of different monomers, the thickness of each layer is almost equal, so we can estimate the natural period by calculating the average thickness of each layer. Through our calculation, the natural period L_0 approaches to 7.5.

Next, we study the effect of the confinement degree d on the morphology of the mixture. We regulate the distance between walls from 128 to 80, and figure 8 shows the evolution patterns for $f = 51.7/48.3$ under different confinement degrees. In this part, the walls are neutral, and the value of parameter b_{11} is 0.099.

From Fig. 8 we can see that when the walls are neutral, if the ratio of d/L_0 is an integer, in other words, the distance between walls is commensurate with the natural period of the mixture, the effect of walls confinement is weak, and the morphology is similar to the bulk, the macrophase is isotropic. When the ratio is not an integer, that is to say, the distance between walls is incommensurate with the natural period, the effect on the morphology is obvious, and the morphology becomes ordered and perpendicular to the walls. As a result, the patterns display periodic oscillation with the distance between walls decreasing. We can easily understand the reason for this result: when the distance between walls is commensurate with the natural period of the mixture, the chains of the copolymers can extend in any direction, so the macro-morphology is isotropic; but when the distance between walls is incommensurate with the natural period, the extension of copolymer chains is restricted by the walls, so the chains tend to unfold along the direction of the walls, resulting in the striped structures in the whole range. On the other hand, the reinforcing of the confinement effect leads to an increase of free energy, so the system entropy decreases and an ordered structure forms in the end.

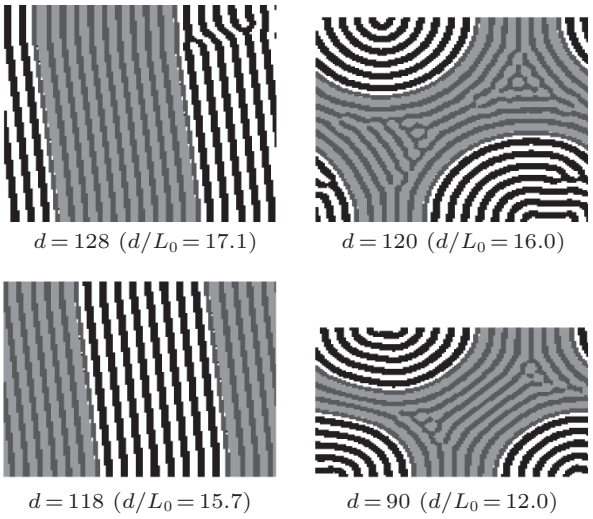


Fig. 8. Domain patterns for $f = 51.7/48.3$ and $b_{11} = 0.099$ at $t = 5 \times 10^6$ with different confinement degree d. The color details are the same as those in Fig. 1.

In addition, we can also see that with the distance between walls reducing, the macrolayer structure increases, so we can predict that if we reduce the distance between walls continuously, we can get a multiple layer structure perpendicular to the walls with the alternating of *AB*-rich and *CD*-rich microdomains.

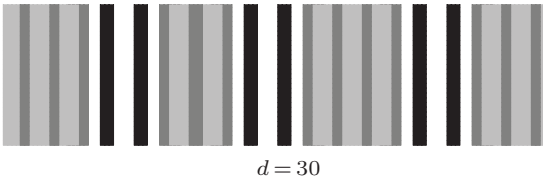


Fig. 9. Domain pattern for $b_{11} = 0.099$ at $t = 5 \times 10^6$ with $d = 30$. The color details are the same as those in Fig. 1.

Figure 9 shows that when the distance between walls is small enough ($d = 30$), which means that the confinement degree is strong enough, a multilayered structure appears in the mixture. The reason for this result is that when the distance between walls is very small, the effect of confinement enhances, so that the copolymer chains cannot move in the whole range and the mixture cannot separate into two parts completely, so a multilayered structure occurs in the system.

4. Conclusion

In this paper, we have investigated the phase behaviors in a binary mixture of diblock copolymers confined between two parallel walls by using cell dynamics simulation of the time-dependent Ginzburg–Landau theory. The morphological dependence of the wall–block interaction and the confinement degree has been systematically studied and the repulsive interactions between different monomers are also discussed.

From the simulation, we find that much richer morphologies can form in the asymmetric binary mixture of diblock copolymers than in the pure diblock copolymer. We observed the orientational transitions in the perfect striped sandwich structures in the mixture, while it was not observed in the pure diblock copolymer. When the wall–block interaction increases, the morphology of the mixture changes from isotropic to the state perpendicular to the walls, and then to the state parallel to the walls. When the repulsive interactions between different monomers decrease, the *CD* copolymer transits from parallel to the macrophase interfaces to perpendicular to the interfaces, resulting in the different morphologies of the sandwich structures. When the distance between walls decreases, the morphologies of the mixture display periodic oscillation between isotropic and perpendicular states, and we get multiple layer structures when the confinement degree is strong enough. It is worth mentioning that Matsen[13] has already predicted that the mixture of different copolymers would display more complex morphology when they are confined between two parallel walls, and he developed a numerical method for examining complex morphologies in thin films of block copolymer, and evaluated the stability of parallel, perpendicular, and mixed lamella phases. Interestingly, our results are just in agreement with his conclusion, and a series of special morphologies were observed in our work.

Furthermore, for the interesting multiple layer sandwich structures, we discussed the parametric dependence and physical reasons for the microdomain growth and orientational order transitions. We have examined in detail the formation process and domain growth of the *AB* diblock copolymer striped structure. The wall–block interaction, wall confinement degree, and the strong repulsive interactions between different monomers play an important role in the formation of striped structures and the orientational transitions. It is expected that the efficient values of the interactions are also related to the other parameters of the system. Our results may provide guidance for experimentalists, and the model system can also give a simple way to realize orientational order transition in soft materials through parallel wall confinement.

References

[1] Matsen M W and Schickf M 1996 *Current Opinion in Colloid Interface Science* **1** 329
[2] Urbas A, Sharp R, Fink Y, Thomas E L, Xenidou M and Fetters L J 2000 *Adv. Mater.* **12** 812
[3] Hamley I W 2003 *Nanotechnology* **14** R39
[4] Park C, Yoon J and Thomas E L 2003 *Polymer* **44** 6725
[5] Knoll A, Magerle R and Krausch G 2004 *J. Chem. Phys.* **120** 1105
[6] Cong Y, Li B Y, Han Y C, Li Y G and Pan C Y 2005 *Macromolecules* **38** 9836
[7] Bates F S, Maurer W, Lodge T P, Schulz M F, Matsen M W, Almdal K and Mortensen K 1995 *Phys. Rev. Lett.* **75** 4429
[8] Zhao J, Majumdar B, Schulz M F, Bates F S, Almdal K, Mortensen K, Hajduk D A and Gruner S M 1996 *Macromolecules* **29** 1204
[9] Tanaka H, Hasegawa H and Hashimoto T 1991 *Macromolecules* **24** 240
[10] Park D W and Roe R J 1991 *Macromolecules* **24** 5324
[11] Hashimoto T, Koizumi S and Hasegawa H 1994 *Macromolecules* **27** 1562
[12] Rong L X, Wei L H, Dong B Z, Hong X G, Li F M and Li Z C 2003 *Chin. Phys.* **12** 771
[13] Matsen M W 1997 *J. Chem. Phys.* **106** 7781
[14] Chen H Y and Ruckenstein E 2012 *Soft Matter* **8** 1327
[15] Sakurai S and Nomura S 1997 *Polymer* **38** 4103
[16] Likhtman A E and Semenov A N 1997 *Macromolecules* **30** 7273
[17] Kawakatsu T 1994 *Phys. Rev.* E **50** 2856
[18] Zhang J J, Jin G J and Ma Y Q 2006 *J. Phys.: Condens. Matter* **18** 837
[19] Sakurai S 2008 *Polymer* **49** 2781
[20] Matsen M W 2006 *Soft Matter* **2** 1048
[21] Zhang J J, Jin G J and Ma Y Q 2005 *Phys. Rev.* E **71** 051803
[22] Sun M N, Zhang J J, Wang B F, Wu H S and Pan J X 2011 *Phys. Rev.* E **84** 011802
[23] Xu T, Craig J H and Russell T P 2003 *Macromolecules* **36** 6178
[24] Boker A, Schmidt K, Knoll A, Zettl H, Hansel H, Urban V, Abetz V and Krausch G 2006 *Polymer* **47** 849
[25] Schmidt K, Boker A, Zettl H, Schubert F, Hañsel H, Fischer F, Weiss T M, Abetz V, Zvelindovsky A V, Sevink G J A and Krausch G 2005 *Langmuir* **21** 11974
[26] Pinna M and Zvelindovsky A V 2008 *Soft Matter* **4** 316
[27] Hong Y R, Admson D H, Chainkin P M and Register R A 2009 *Soft Matter* **5** 1687
[28] Morozov A N, Zvelindovsky A V and Fraaije J G E M 2000 *Phys. Rev.* E **61** 4125
[29] Morozov A N, Zvelindovsky A V and Fraaije J G E M 2001 *Phys. Rev.* E **64** 051803
[30] Morozov A N and Fraaije J G E M 2002 *Phys. Rev.* E **65** 031803
[31] Ludovic Berthier 2001 *Phys. Rev.* E **63** 051503
[32] Böltau M, Walheim S, Mlynek J, Krausch G and Steiner U 1998 *Nature* **391** 877
[33] Tsarkova L, Knoll A, Krausch G and Magerle R 2006 *Macromolecules* **39** 3608
[34] Zhang J J, Jin G J and Ma Y Q 2005 *Eur. Phys. J.* E **18** 359
[35] Puri S and Binder K 1994 *Phys. Rev.* E **49** 5359
[36] Chen H Y, Peng C J, Sun L, Liu H L and Hu Y 2007 *Langmuir* **23** 11112
[37] Chen H Y, Chen X Q, Ye Z C, Liu H L and Hu Y 2010 *Langmuir* **26** 6663
[38] Wang X H, Li S B, Zhang L X and Liang H J 2011 *Chin. Phys.* B **20** 083601
[39] Kikuchi M and Binder K 1994 *J. Chem. Phys.* **101** 3367
[40] Varnik F, Baschnagel J and Binder K 2000 *J. Chem. Phys.* **113** 4444
[41] Ausserré D 1989 *J. Phys. France* **50** 3021
[42] Aoyagi T, Takimoto Junichi and Doi M 2001 *J. Chem. Phys.* **115** 552
[43] Xia J F, Wang J, Lin Z Q, Qiu F and Yang Y L 2006 *Macromolecules* **39** 2247

[44] Hsu H P and Grassberger P 2004 *J. Chem. Phys.* **120** 2034
[45] Kellogg G J, Walton D G, Mayes A M, Lambooy P, Russell T P, Gallagher P D and Satija S K 1996 *Phys. Rev. Lett.* **76** 2503
[46] Koneripalli N, Levickt R, Bates F S, Ankner J, Kaiser H and Satija S K 1996 *Langmuir* **12** 6681
[47] Lambooy P, Russell T P, Kellogg G J, Mayes A M, Gallagher P D and Satija S K 1994 *Phys. Rev. Lett.* **72** 2899
[48] Chen H and Chakrabati A 1998 *J. Chem. Phys.* **108** 6897
[49] Pickett G T and Balazs A C 1997 *Macromolecules* **30** 3097
[50] Wang Q, Yan Q, Nealey P F and de Pablo J J 2000 *J. Chem. Phys.* **112** 450
[51] Wang Q, Nealey P F and de Pablo J J 2001 *Macromolecules* **34** 3458
[52] Feng J, Liu H L and Hu Y 2002 *Macromol. Theor. Simul.* **11** 549
[53] Feng J, Liu H L and Hu Y 2002 *Macromol. Theor. Simul.* **11** 556
[54] Yin Y H, Jiang R, Li B H, Chen T H, Jin Q H, Ding D T and Shi A C 2006 *J. Chem. Phys.* **124** 184708
[55] Turner M S 1992 *Phys. Rev. Lett.* **69** 1788
[56] Li Y Y, Zhou Y and Zhang G Z 2006 *Chin. Phys.* **15** 985
[57] Han Y Y, Cui J and Jiang W 2008 *Macromolecules* **41** 6239
[58] Zhu Y T and Jiang W 2007 *Macromolecules* **40** 2872
[59] Wilms D, Winkler A, Virnau P and Binder K 2010 *Phys. Rev. Lett.* **105** 045701
[60] Chen H Y and Ruckenstein E 2009 *Langmuir* **25** 12315
[61] Chen H Y and Ruckenstein E 2010 *Polymer* **51** 968
[62] Liu M J, Li S B, Zhang L X and Wang X H 2010 *Chin. Phys.* B **19** 028101
[63] Feng J and Ruckenstein E 2006 *Macromolecules* **39** 4899
[64] Sevink G J A, Zvelindovsky A V, Fraaije J G E M and Huinink H P 2001 *J. Chem. Phys.* **115** 8226
[65] Yu B, Sun P C, Chen T H, Jin Q H, Ding D T, Li B H and Shi A C 2006 *Phys. Rev. Lett.* **96** 138306
[66] Wang Z, Li B H, Jin Q H, Ding D T and Shi A C 2008 *Macromol. Theor. Simul.* **17** 301
[67] Ma M L, Thomas E L, Rutledge G C, Yu B, Li B H, Jin Q H, Ding D T and Shi A C 2010 *Macromolecules* **43** 3061
[68] Kalra V, Mendez S, Lee J H, Nguyen H, Marquez M and Joo Y L 2006 *Adv. Mater.* **18** 3299
[69] Wu Y Y, Cheng G S, Katsov K, Sides S W, Wang J F, Tang J, Fredrickson G H, Moskovits M and Stucky G D 2004 *Nat. Mater.* **3** 816
[70] Pinna M, Guo X H and Zvelindovsky A V 2009 *J. Chem. Phys.* **131** 214902
[71] Arsenault A C, Rider D A, Tétreault N, Chen J I L, Coombs N, Ozin G A and Manners I 2005 *J. Am. Chem. Soc.* **127** 9954
[72] Yu B, Li B H, Jin Q H, Ding D T and Shi A C 2007 *Macromolecules* **40** 9133
[73] Pinna M, Hiltl S, Guo X H, Böker A and Zvelindovsky A V 2010 *ACS Nano* **4** 2845
[74] Tang P, Qiu F, Zhang H D and Yang Y L 2005 *Phys. Rev.* E **72** 016710
[75] Rider D A, Chen J I L, Eloi J C, Arsenault A C, Russell T P, Ozin G A and Manners I 2008 *Macromolecules* **41** 2250
[76] Oono Y and Puri S 1987 *Phys. Rev. Lett.* **58** 836
[77] Puri S and Oono Y 1988 *Phys. Rev.* A **38** 1542
[78] Oono Y and Puri S 1988 *Phys. Rev.* A **38** 434
[79] Marko J F 1993 *Phys. Rev.* E **48** 2861
[80] Ohta T and Ito A 1995 *Phys. Rev.* E **52** 5250
[81] Ito A 1998 *Phys. Rev.* E **58** 6158
[82] Ohta T and Kawasaki K 1986 *Macromolecules* **19** 2621
[83] Shinozaki A and Oono Y 1993 *Phys. Rev.* E **48** 2622
[84] Martins S, Morgado W A M, Massunaga M S O and Bahiana M 2000 *Phys. Rev.* E **61** 4118
[85] Bates F S and Fredrickson G H 1990 *Ann. Rev. Phys. Chem.* **41** 525